PAPER

GaN directional couplers for on-chip optical interconnect

IOP Publishing Semiconductor Science and Technology
Semicond. Sci. Technol. 32 (2017) 045001 (7pp) https://doi.org/10.1088/1361-6641/aa59ef

GaN directional couplers for on-chip optical interconnect

Jialei Yuan[1], Xumin Gao[1], Yongchao Yang[1], Guixia Zhu[1], Wei Yuan[1], Hoi Wai Choi[2], Zhiyu Zhang[3] and Yongjin Wang[1]

[1] Grünberg Research Centre, Nanjing University of Posts and Telecommunications, Nanjing 210003, People's Republic of China
[2] Department of Electrical and Electronic Engineering, The University of Hong Kong, 999077, Hong Kong, China
[3] Changchun Institute of Optics, Fine Mechanics and Physics, Chinese Academy of Science, Changchun 130033, People's Republic of China

E-mail: wangyj@njupt.edu.cn

Received 23 October 2016, revised 1 December 2016
Accepted for publication 19 December 2016
Published 2 March 2017

Abstract

Here, we propose, fabricate and characterize GaN directional couplers for on-chip optical interconnect on a GaN-on-silicon platform. Suspended InGaN/GaN multiple-quantum-well diodes are adopted for both the transmitter and the receiver, and GaN directional couplers are used to achieve the light coupling between suspended waveguides that are directly connected to the transmitter and the receiver. The proposed on-chip optical interconnects are experimentally demonstrated by light propagation and in-plane data transmission using visible light. The light propagation images directly show that the emitted light can be laterally coupled into the suspended waveguide, and the guided light from the input waveguide then couples to the coupled waveguide due to the overlapped slab. The receiver detects the transmitted light from the coupled waveguide to complete the in-plane visible light communication process, as confirmed by pseudo-random binary sequence data and eye diagrams at the transmission rate of 30 Mbps.

Keywords: directional coupler, on-chip optical interconnect, InGaN/GaN multiple-quantum-well diode, in-plane visible light communication, GaN-on-silicon platform

(Some figures may appear in colour only in the online journal)

Directional couplers are some of the fundamental optical components in a photonic circuit and are used for the coupling of optical power between two waveguides in a given direction of light propagation [1–5]. A directional coupler usually employs parallel, intersecting rib waveguides with their overlapped slab within up to a few microns of the waveguides in the intersection region to permit light transfer between the waveguides. GaN directional couplers have been fabricated on a GaN-on-sapphire platform for integrated quantum photonics [6]. GaN is an excellent optical material for the development of photonic circuits from the visible to the infrared range [7–11]. A higher index contrast can be achieved using a substrate removal technique that is promising for the formation of highly optical confined waveguides. Moreover, an emitter and a detector can be fabricated on a single chip based on an InGaN/GaN multiple-quantum-well diode (MQWD) [12, 13]. On-chip optical interconnects have been extensively investigated [14–16]. Various photonic circuits can be developed for diverse applications by combinations with an emitter, a waveguide, a coupler and a detector on a chip [17, 18].

Here, we propose, fabricate and characterize a photonic integration of an InGaN/GaN MQWD, a suspended GaN waveguide and a directional coupler on a GaN-on-silicon platform, leading to the formation of on-chip optical interconnects. Using a combination of silicon removal and back wafer etching of suspended epitaxial films, a highly optically confined GaN waveguide and a directional coupler are generated by exploiting the large index contrast between GaN and air [19]. Suspended InGaN/GaN MQWDs are used for

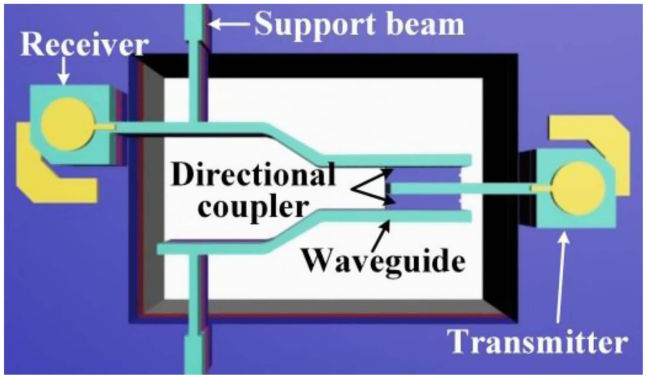

Figure 1. Schematic of proposed on-chip optical interconnects made with suspended GaN directional coupler.

both the transmitter and the receiver in the in-plane visible light communication (VLC) system and are fabricated by identical processes. In the GaN directional coupler, the light power and fields of one waveguide interact with the light power and fields of another waveguide, coupling signals from one waveguide to another to complete the in-plane data transmission. Light propagation images are measured to directly characterize the light coupling, and the in-plane VLC process is experimentally demonstrated by the transmission and detection of pseudo-random binary sequence (PRBS) data and eye diagrams.

Figure 1 shows a schematic of our proposed on-chip optical interconnects made with suspended GaN directional coupler. The InGaN/GaN MQWD at the right top corner is adopted as the detector (receiver) when acting as a photodiode to sense the light, and another InGaN/GaN MQWD at the left bottom corner is used as the emitter (transmitter) when it serves as a light-emitting diode to emit the modulated light. The in-plane confined light of the emitter is first coupled into the suspended waveguide that is parallel to the InGaN/GaN MQWD surface and is used as the input port of the directional coupler. The light couples to another waveguide to propagate to the coupled port of the directional coupler due to the overlapped slab in the directional coupler region. Hence, the in-plane light propagation between the detector and the emitter is created through the suspended waveguides, leading to an in-plane signal transmission using visible light. Moreover, another coupled waveguide is fabricated for reference.

The on-chip photonic integration of suspended InGaN/GaN MQWDs, a waveguide and directional coupler is implemented on a 2-inch GaN-on-silicon wafer [20–22]. The growth of GaN-on-silicon InGaN/GaN MQWD structures is conducted out with a metal–organic chemical vapor phase deposition [23–25], and Al-composition step-graded AlGaN multilayers are sandwiched between GaN and silicon substrate for stress management [26–28]. The heat dissipation issue can be addressed through the growth on metallic substrate [29]. For the subsequent silicon removal, the 1500 μm-thick silicon substrate is first thinned to 200 μm by chemical-mechanical polishing. The top epitaxial layers consist of an 80 nm-thick p-type Mg-doped GaN layer, a 35 nm-thick p-type Mg-doped AlGaN layer, a 120 nm-thick InGaN/GaN MQWs, a 3400 nm-thick n-type Si-doped GaN layer, a 400 nm-thick undoped GaN layer, a 600 nm-thick AlGaN buffer layer and a 330 nm-thick AlN layer. The top layer is defined by photolithography and is etched down to n-type Si-doped GaN to form mesa by inductively coupled plasma reactive ion etching (ICP RIE) with Cl_2 and BCl_3 hybrid gases at the flow rates of 10 sccm and 25 sccm, respectively. The etch rate is approximately 120 nm min^{-1}, and the 1.6 μm-thick AZ5214 photoresist serves as the etching hard mask. Subsequently, the 20 nm Ni/180 nm Au bilayers are evaporated onto the surface of the p-GaN and the n-GaN layers as the metal electrodes. After the lift-off process, the sample is annealed at 500 °C in an N_2 atmosphere for 5 min to obtain p- and n-contacts, leading to the formation of InGaN/GaN MQWDs. The directional coupling regions are then patterned and etched to the depth of ~1 μm by ICP RIE, where the 1.6 μm-thick AZ5214 photoresist serves as the etching hard mask. The 6.7 μm-thick AZ4620 photoresist serves as the etching hard mask for long time etching of GaN because it is a hard material [30–32]. The supporting arms and waveguides are then patterned and etched at the depth of ~3 μm by ICP RIE. The top device structures are protected by the 6.7 μm-thick AZ4620 photoresist, and the silicon substrate is then spin-coated with the 16 μm-thick AZ4620 photoresist and patterned by backside alignment photolithography. Silicon removal is conducted to obtain suspended device architecture,

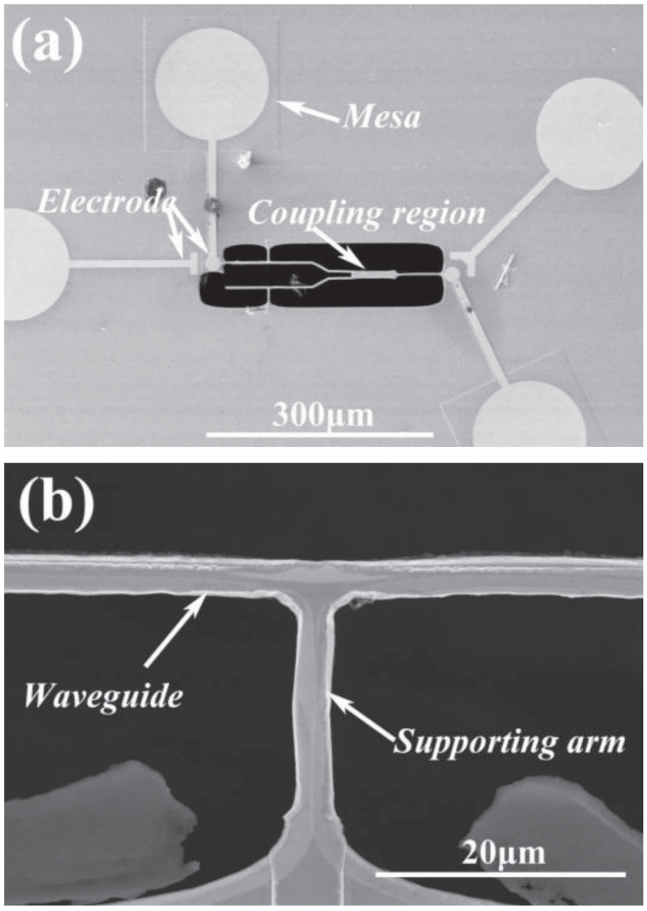

Figure 2. (a) SEM image of the on-chip optical interconnects featured with a GaN directional coupler. (b) High magnification image of the SEM image of the supporting part.

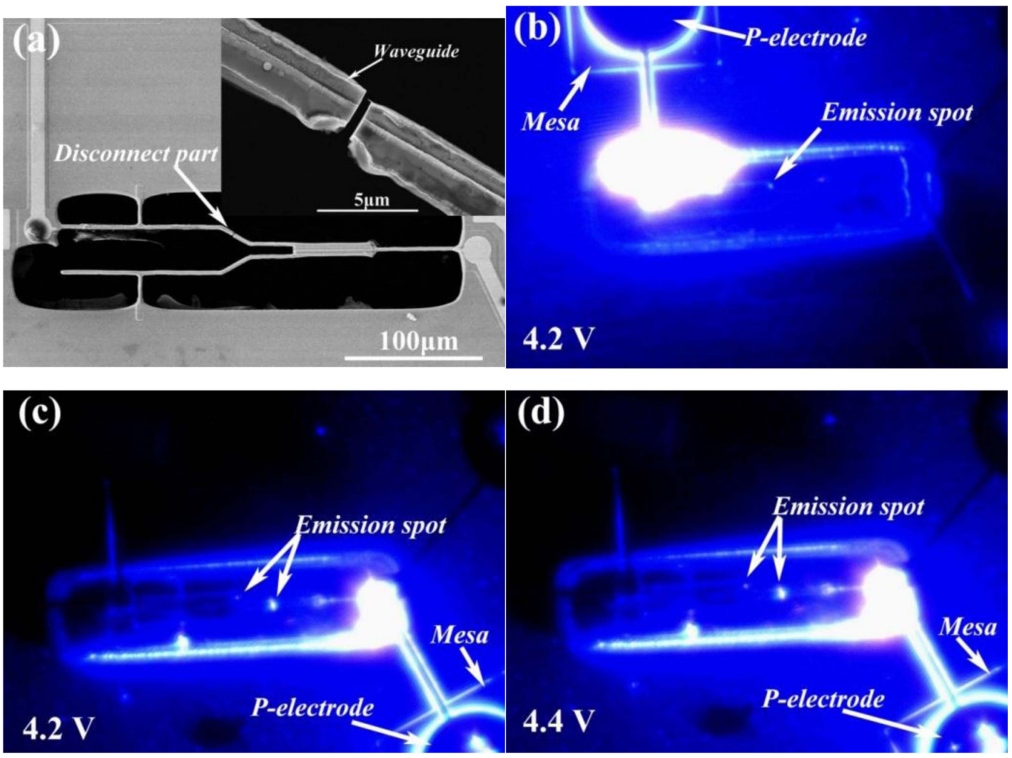

Figure 3. (a) SEM image of an integrated photonic circuit with an inset showing the magnified disconnected part. (b) Measured light propagation images when the left InGaN/GaN MQWD is biased at 4.2 V. (c) and (d) measured light propagation images when the right InGaN/GaN MQWD is biased at 4.2 and 4.4 V, respectively.

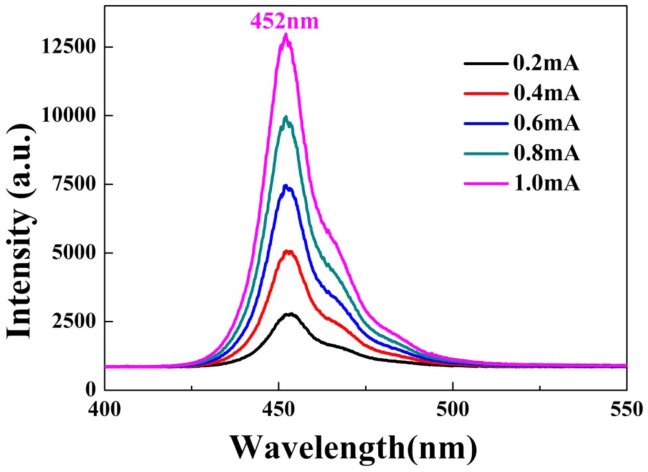

Figure 4. The measured electroluminescence (EL) spectra of light emission.

where the AlN buffer layer acts as the etching stop layer. Suspended epitaxial films are etched from the backside by ICP RIE to obtain ultrathin integrated devices on the 2 μm-thick self-supported membrane.

Figure 2(a) shows the scanning electron microscope (SEM) image of the on-chip optical interconnects made with a GaN directional coupler. The coupling length of the directional coupler is 60 μm. In the directional coupler region, the suspended rectangular waveguides are replaced by suspended rib waveguides, where the waveguide rib etch depth is 1 μm, and the thickness of the overlapped slab is 1 μm. The optical modes spread horizontally into the underlying slab, leading to the mode overlap for the light coupling between the input waveguide and the coupled waveguide. The overlapped slab also has the supporting functionality for an integrated photonic circuit. The 1.5 μm-wide, 1 μm-high and 60 μm-long isolation trenches are formed by ICP-RIE to separate the p-GaN layers for the transmitter and the receiver. The 60 μm-long, 3 μm-wide and 2 μm-high waveguide is connected to the directional coupler and one InGaN/GaN MQWD. At the other end of the GaN directional coupler, two semi-Y-branch waveguides with a length, width and height of 140 μm, 3 μm and 2 μm, respectively, are used. One semi-Y-branch waveguide impinges on another InGaN/GaN MQWD, and the other semi-Y-branch waveguide is used for reference. Figure 2(b) shows a high magnification image of the supporting arms, which are used to address the fracture issue of suspended waveguides [33]. The strain relaxation during etching process, which also affects the emission wavelength [34], can be managed to obtain a suspended device architecture. Device deviations from the ideal elements are attributed to the misalignment and ICP RIE processes. It is possible to further optimize the fabrication processes to decrease deviations between the fabricated devices and the designed elements. It is possible to further optimize the fabrication processes to decrease the deviations between the fabricated devices and the designed elements.

The InGaN/GaN MQWD is assumed to uniformly emit light in all directions so that the in-plane confined light could be laterally coupled into the suspended waveguide that is

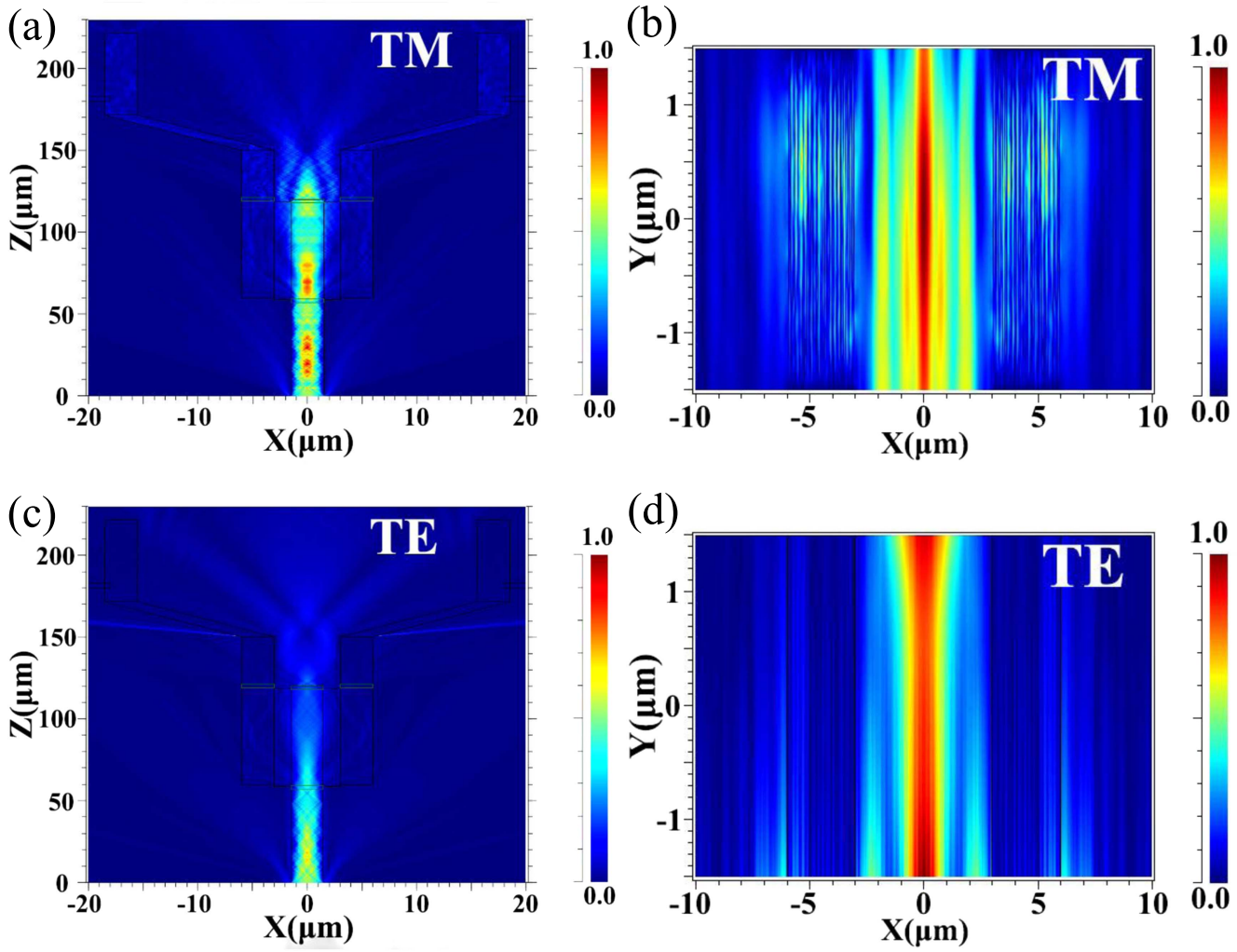

Figure 5. The light propagation inside the suspended photonic circuit: (a) the plan view of TM-polarized light; (b) field profile with a coupling length of 59 μm; (c) the plan view of TE-polarized light; (b) field profile with a coupling length of 59 μm.

directly connected to the InGaN/GaN MQWD regarded as the transmitter. Figure 3(a) shows a SEM image of the integrated photonic circuit, where one semi-Y-branch waveguide is broken. The disconnected part is magnified in the inset of figure 3(a) and can be used as a waveguide output port, endowing the capability to directly observe the light propagation performance of the photonic circuit. As shown in figure 3(b), the emitted light from the InGaN/GaN MQWD is laterally coupled into the suspended waveguide and then guided along the semi-Y-branch waveguide when the InGaN/GaN MQWD is biased at 4.0 V. At the disconnect region, the guided light is diffracted into the air at the waveguide output facet. Correspondingly, the emitted light is laterally coupled into the suspended straight waveguide when another InGaN/GaN MQWD is biased at 4.2 V, as shown in figure 3(c). The guided light coupling between the input waveguide and the coupled waveguides occurs in the directional coupler region. The coupled light is then guided by the coupled waveguides and diffracted into air at the waveguide output facets, as confirmed by the light emission spots. Moreover, a light emission spot can be clearly observed at the output port of the directional coupler. Figure 3(d) shows that the light emission is improved as the bias voltage is increased to 4.4 V. Hence, more light power is transferred to the input waveguide. As a result, the light spots at the coupled waveguide facets become brighter. This means that the light intensity can be tuned by the bias voltage, which is essential for the VLC system [35, 36].

The EL spectra at different injection currents of the InGaN/GaN MQWD are measured using an Ocean Optics USB4000 spectrometer. Figure 4 shows the measured the EL spectra of the light emission. The peak emission wavelength locates around 452 nm, and the directional coupler allows broad band coupling compared with the waveguide architecture. The light emission intensity is tuned by the injection current, which agrees well with the light propagation observation.

A simulation of the integrated directional coupler is performed using the RSoft BeamPROP mode solver. The used effective refractive index of the suspended waveguide is 2.45 and the surrounding medium is air. A 452 nm circularly symmetric Gaussian beam is adopted for simulation. The middle straight waveguide is 3 μm thick and 3 μm wide. In the coupling region, the coupling gaps between the coupled

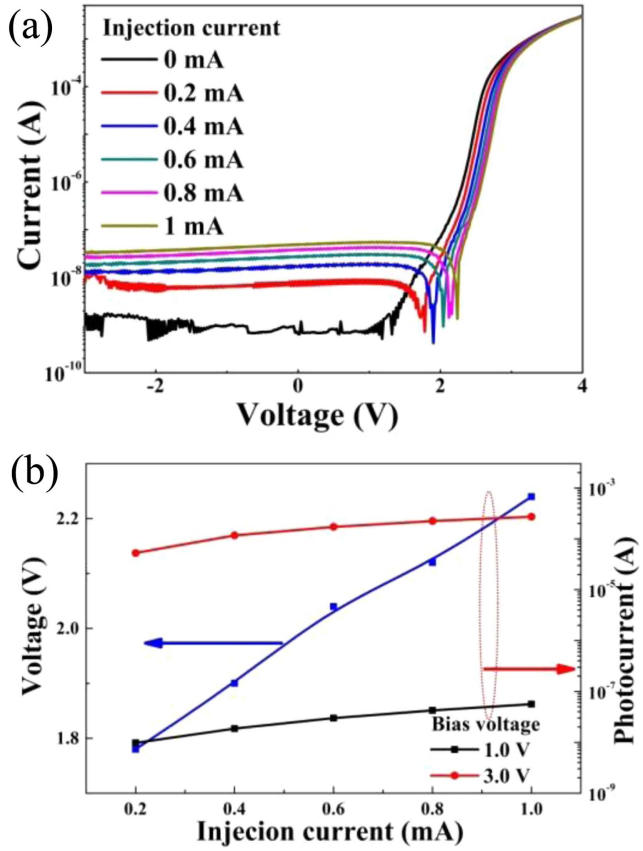

Figure 6. (a) Log-scaled *I–V* plots for the receiver as a function of the injection current of the transmitter. (b) Dip shifts and induced photocurrent versus the injection current of the transmitter.

waveguide and the middle straight waveguide are 1.5 μm. The rib height is 1 μm and the underlying layer is 2 μm thick. Figure 5(a) illustrates the plan view simulation with transverse-magnetic (TM) polarization mode. The light power is transformed from the middle waveguide to the coupled waveguides. Figure 5(b) shows the overlapped optical modes in the TM field profile observed at 119 μm, which has a coupling length of 59 μm. The transverse-electric (TE) polarized light propagation inside directional coupler is illustrated in figure 5(c), and the field profile at 119 μm shows the overlapped optical modes. The light coupling is obtained through the underlying layer and can be improved by increasing the coupling length or decreasing the coupling gap.

As the receiver, the InGaN/GaN MQWD detects the incident light and completes the photon-to-electron conversion so that the induced photocurrent depends on the light intensity. On the other hand, the InGaN/GaN MQWD emits the modulated light to generate the electron-to-photon conversion when it acts as the transmitter. The emitted light intensity is controlled by the injection current. Therefore, in our proposed in-plane VLC system, the current-voltage (*I–V*) performance at the receiver is tuned by the light guided through the suspended waveguides that is modulated by the injection current at the transmitter. Figure 6(a) shows the log-scaled *I–V* plots for the receiver as a function of the injection current of the transmitter. The measured currents are the sum of the induced photocurrent and the driven current that flow in opposite directions. It can be clearly observed that the *I–V* performance at the receiver is influenced by the injection current of the transmitter. The receiver absorbs much more light power with the increasing injection current of the transmitter, leading to a higher amplitude of the induced photocurrent. The induced photocurrents are equal to the driven currents around the sharp dips. The measured current values at the injection current of 0 mA for the transmitter are subtracted from the measured current values to obtain the induced photocurrents. When the induced photocurrent is

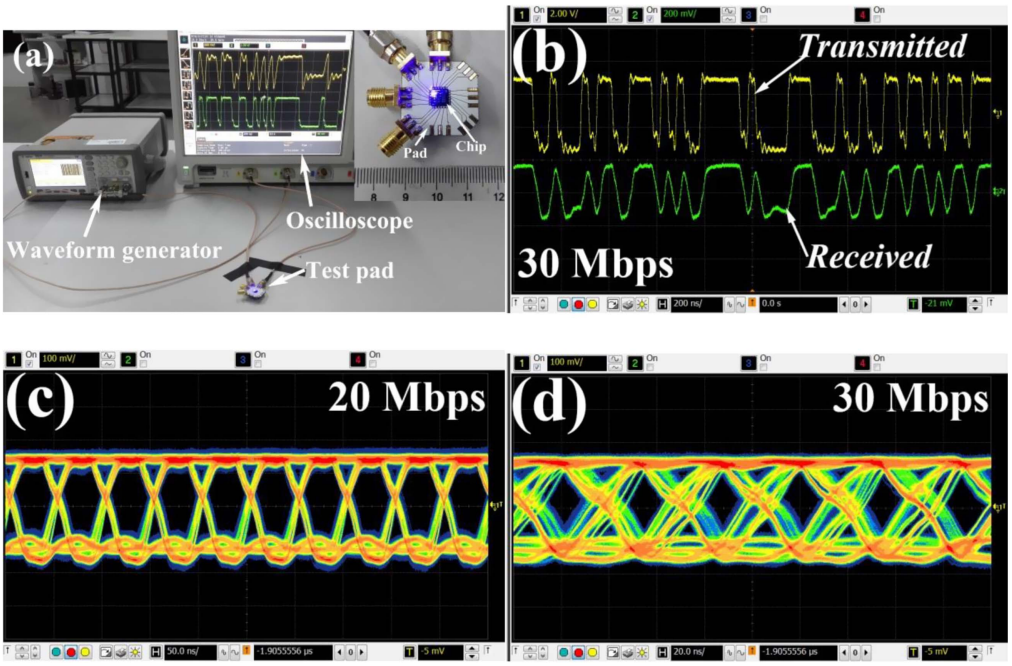

Figure 7. (a) Wire-bonded chip. (b) Measured PRBS data at a transmission rate of 30 Mbps. (c) and (d) eye diagrams measured at transmission rates of 20 and 30 Mbps, respectively.

equal to the driven current at the receiver, a distinct sharp dip occurs. As illustrated by the blue line in figure 6(b), the sharp dip is tuned by the injection current of the transmitter and shifts to higher forward voltage of the receiver. The induced photocurrent increases when the injection current of the transmitter increases. The receiver simultaneously detects and emits light when the InGaN/GaN MQWD is biased at 3.0 V, and the induced photocurrent is greatly increased compared with that measured at a bias voltage of 1.0 V.

Figure 7(a) shows the wire-bonded chip, which is separated from the processed wafer and fixed to a test pad for device characterization. The input port is directly connected to an Agilent 33522A arbitrary waveform generator to generate the modulated light, and the output port is connected to an Agilent DSO9254A digital storage oscilloscope. The transmission and detection of PRBS data are performed to confirm the in-plane information process using visible light. Figure 7(b) shows the transmitted and received PRBS data for the wire-bonded chip at the transmission rate of 30 Mbps. The receiver is biased at 0.0 V and only serves as a photodiode. The measured bit patterns confirm that the integrated photonic circuit featuring GaN directional coupler can transmit and detect PRBS data for the in-plane visible light communication. Compared to the transmitted/received signals, the signals suffer waveform distortions due to light propagation through a band-limited channel. The transmission rate could be further improved with implementation of nano-LEDs by decreasing the p-electrode size [37, 38]. Figure 7(c) shows the measured eye diagrams obtained at the transmission rate of 20 Mbps; these are considered to be wide open. As the transmission rate increases, the waveform distortion increases. Hence, the eye begins to close as the data rate increases to 30 Mbps, as shown in figure 7(d).

In conclusion, we have proposed and fabricated GaN directional couplers for on-chip optical interconnect on a GaN-on-silicon platform, in which suspended MQWDs are adopted for both the transmitter and the receiver. A GaN directional coupler is used to achieve the light coupling between two suspended waveguides, connected to the transmitter and the receiver. Light power is partially transferred from the input waveguide to the coupled waveguide through the directional coupler, as directly confirmed by the light propagation images. The in-plane communication process using visible light is experimentally demonstrated by the transmission and detection of PRBS data and eye diagrams at the transmission rate of 30 Mbps.

Acknowledgments

We thank the Grünberg Research Centre for the use of their equipment. The work is jointly supported by the National Natural Science Foundation of China (grant nos. 61322112 and 61531166004), research Projects (nos. 2014CB360507 and S2016G6424), and the Natural Science Foundation of Jiangsu Province (BE2016186).

References

[1] Mercatili E A J 1969 Dielectric rectangular waveguide and directional coupler for integrated optics *Bell Syst. Tech. J.* **48** 2071
[2] Streltsov A M and Borrelli N F 2001 Fabrication and analysis of a directional coupler written in glass by nanojoule femtosecond laser pulses *Opt. Lett.* **26** 42–3
[3] Thompson M, Politi A, Matthews J and O'Brien J 2011 Integrated waveguide circuits for optical quantum computing *IET Circuits, Devices & Systems* **5** 94
[4] Lu Z Q, Yun H, Wang Y, Chen Z T, Zhang F, Jaeger N A F and Chrostowski L 2015 Broadband silicon photonic directional coupler using asymmetric-waveguide based phase control *Opt. Express* **23** 3795–808
[5] Sun Y, Xiong Y L and Ye W N 2016 Experimental demonstration of a two-mode (de)multiplexer based on a taper-etched directional coupler *Opt. Lett.* **41** 3743–6
[6] Zhang Y, McKnight L, Engin E, Watson I M, Cryan M J, Gu E, Thompson M G, Calvez S, O'Brien J L and Dawson M D 2011 GaN directional couplers for integrated quantum photonics *Appl. Phys. Lett.* **99** 161119
[7] Dharanipathy U, Vico Triviño N, Yan C, Diao Z, Carlin J-F, Grandjean N and Houdré R 2012 Near-infrared characterization of gallium nitride photonic-crystal waveguides and cavities *Opt. Lett.* **37** 4588–90
[8] Bruch A W, Xiong C, Leung B, Poot M, Han J and Tang H X 2015 Broadband nanophotonic waveguides and resonators based on epitaxial GaN thin films *Appl. Phys. Lett.* **107** 141113
[9] Roland I *et al* 2016 Near-infrared III-nitride-on-silicon nanophotonic platform with microdisk resonators *Opt. Express* **24** 9602–10
[10] Shokhovets S, Himmerlich M, Kirste L, Leach J H and Krischok S 2015 Birefringence and refractive indices of wurtzite GaN in the transparency range *Appl. Phys. Lett.* **107** 092104
[11] Sun Y *et al* 2016 Room-temperature continuous-wave electrically injected InGaN-based laser directly grown on Si *Nat. Photon.* **10** 595–9
[12] Li X, Zhu G, Gao X, Bai D, Huang X, Cao X, Zhu H, Hane K and Wang Y 2015 Suspended p-n Junction InGaN/GaN multiple-quantum-well device with selectable functionality *IEEE Photon. J.* **7** 1–7
[13] Mikulics M, Marso M, Javorka P, Kordoš P, Lüth H, Kočan M, Rizzi A, Wu S and Sobolewski R 2005 Ultrafast metal-semiconductor-metal photodetectors on low-temperature-grown GaN *Appl. Phys. Lett.* **86** 211110
[14] Xiong C, Pernice W H P and Tang H X 2012 Low-loss, silicon integrated, aluminum nitride photonic circuits and their use for electro-optic signal processing *Nano Lett.* **12** 3562–8
[15] Eggleston M S and Wu M C 2015 Efficient coupling of an antenna-enhanced nanoLED into an integrated InP waveguide *Nano Lett.* **15** 3329–33
[16] Petykiewicz J, Nam D, Sukhdeo D S, Gupta S, Buckley S, Piggott A Y, Vučković J and Saraswat K C 2016 Direct bandgap light emission from strained germanium nanowires coupled with high-Q nanophotonic cavities *Nano Lett.* **16** 2168–73
[17] Brubaker M D, Blanchard P T, Schlager J B, Sanders A W, Roshko A, Du S M, Gray J M, Bright V M, Sanford N A and Bertness K A 2013 On-chip optical interconnects made with gallium nitride nanowires *Nano Lett.* **13** 374–7
[18] Tchernycheva M *et al* 2014 Integrated photonic platform based on InGaN/GaN nanowire emitters and detectors *Nano Lett.* **14** 3515–20
[19] Triviño N V, Butte R, Jean-Francois Carlin J-F and Grandjean N 2015 Continuous wave blue lasing in III-nitride nanobeam cavity on silicon *Nano Lett.* **15** 1259–63

[20] Cai W, Yang Y C, Gao X M, Yuan J L, Yuan W, Zhu H B and Wang Y 2016 On-chip integration of suspended InGaN/GaN multiple-quantum-well devices with versatile functionalities *Opt. Express* **24** 6004–10
[21] Wang Y J, Zhu G X, Cai W, Gao X M, Yang Y C, Yuan J L, Shi Z and Zhu H B 2016 On-chip photonic system using suspended p-n junction InGaN/GaN multiple quantum wells device and multiple waveguides *Appl. Phys. Lett.* **108** 162102
[22] Wang Y J, Xu Y, Yang Y C, Gao X M, Zhu B C, Cai W, Yuan J L, Zhang R and Zhu H B 2017 Simultaneous light emission and detection of InGaN/GaN multiple quantum well diodes for in-plane visible light communication on a chip *Opt. Commun.* **387** 440–5
[23] Hardtdegen H, Hollfelder M, Meyer R, Carius R, Münder H, Frohnhoff S, Szynka D and Lüth H 1992 MOVPE growth of GaAs using a N_2 carrier *J. Cryst. Growth* **124** 420
[24] Hardtdegen H, Pristovsek M, Menhal H, Zettler J-T, Richter W and Schmitz D 1998 *In situ* characterization of GaAs growth in nitrogen atmosphere during MOVPE: a comparison to hydrogen atmosphere *J. Cryst. Growth* **195** 211
[25] Cho Y S, Hardtdegen H, Kaluza N, Thillosen N, Steins R, Sofer Z and Lüth H 2006 Effect of carrier gas on GaN epilayer characteristics *Phys. Status Solidi* **3** 1408
[26] Contreras O, Ponce F A, Christen J, Dadgar A and Krost A 2002 Dislocation annihilation by silicon delta-doping in GaN epitaxy on Si *Appl. Phys. Lett.* **81** 4712
[27] Dadgar A, Hums C, Diez A, Bläsing J and Krost A 2006 Growth of blue GaN LED structures on 150 mm Si(1 1 1) *J. Cryst. Growth* **297** 279–82
[28] Sun Y *et al* 2016 Room-temperature continuous-wave electrically injected InGaN-based laser directly grown on Si *Nature Photon.* **10** 595–9
[29] Mikulics M, Kočan M, Rizzi A, Javorka P, Sofer Z, Stejskal J, Marso M, Kordoš P and Lüth H 2005 Growth and properties of GaN and AlN layers on silver substrates *Appl. Phys. Lett.* **87** 212109
[30] Mikulics M, Hardtdegen H, Gregušová D, Sofer Z, Šimek P, Trellenkamp S, Grützmacher D, Lüth H, Kordoš P and Marso M 2012 Non-uniform distribution of induced strain in a gate-recessed AlGaN/GaN structure evaluated by micro-PL measurements *Semicond. Sci. Technol.* **27** 105008
[31] Mikulics M, Hardtdegen H, Winden A, Fox A, Marso M, Sofer Z, Lüth H, Grützmacher D and Kordoš P 2012 Residual strain in recessed AlGaN/GaN heterostructure field-effect transistors evaluated by micro photoluminescence measurements *Phys. Status Solidi* **9** 911
[32] Mikulics M and Hardtdegen H 2015 Nano-LED array fabrication suitable for future single photon lithography *Nanotechnology* **26** 185302
[33] Mikulics M *et al* 2016 Direct electro-optical pumping for hybrid CdSe nanocrystal/III-nitride based nano-light-emitting diodes *Appl. Phys. Lett.* **108** 61107
[34] Sekiya T, Sasaki T and Hane K 2015 Design, fabrication, and optical characteristics of freestanding GaN waveguides on silicon substrate *J. Vac. Sci. Technol.* B **33** 031207
[35] Minh H L, O'Brien D, Faulkner G, Zeng L, Lee K, Jung D, Oh Y J and Won E T 2009 100 Mb/s NRZ visible light communications using a postequalized white LED *IEEE Photon. Technol. Lett.* **21** 1063–5
[36] Vučić J, Kottke C, Nerreter S, Langer K D and Walewski J W 2010 513 Mbit/s visible light communications link based on DMT-modulation of a white LED *J. Lightw. Technol.* **28** 3512–8
[37] Koester R, Sager D, Quitsch W A, Pfingsten O, Poloczek A, Blumenthal S, Keller G, Prost W, Bacher G and Tegude F-J 2015 High-speed GaN/GaInN nanowire array light-emitting diode on silicon(111) *Nano Lett.* **15** 2318–23
[38] Mikulics M, Winden A, Marso M, Moonshiram A, Lüth H, Grützmacher D and Hardtdegen H 2016 Nano-light-emitting-diodes based on InGaN mesoscopic structures for energy saving optoelectronics *Appl. Phys. Lett.* **109** 41103